

## Scanning-tunneling-microscopy study of Ge/GaAs(110). II. Coalescence and layer-by-layer growth

Y.-N. Yang, Y. S. Luo, and J. H. Weaver

*Department of Materials Science and Chemical Engineering, University of Minnesota, Minneapolis, Minnesota 55455*

(Received 16 June 1992)

Scanning tunneling microscopy has been used to study the postnucleation growth of Ge on GaAs(110) at 420°C. In the deposition range from 1 to 10 monolayers (ML), there is lateral overlayer growth through static coalescence with little change in the island height. For depositions above  $\sim 10$  ML, the surface is completely covered by Ge and layer-by-layer growth is observed. Our results show that rough surfaces with isotropic islands and smooth surfaces with elongated islands can be obtained by simply varying the deposition rate or the growth temperature. Arsenic atom segregation is also observed, and the surface reconstructions reflect the As concentration. We propose a surface structure model consisting of As zigzag chains and As dimers.

### INTRODUCTION

Heterojunctions between semiconductors are of great importance in modern semiconductor technology and a microscopic model of the formation is essential for a detailed understanding of the heterostructure properties.<sup>1,2</sup> The means by which individual islands form on a surface and eventually develop into a complete film can have significant impact on the structural quality of the junction. The Ge/GaAs(110) system is ideal for studies of growth modes. The small lattice mismatch of 0.1% between Ge and GaAs enables epitaxial films to be grown without significant strain. As a result, theoretical modeling of the growth is simplified since only the surface and interfacial free energies need be included in energetic considerations.

Ge/GaAs(110) has been studied extensively using techniques such as Auger electron spectroscopy (AES), photoemission spectroscopy, and low-energy electron diffraction (LEED).<sup>3-8</sup> Epitaxial growth of Ge on GaAs(110) has been reported to occur over a wide temperature range, 160–525°C. These studies have also demonstrated clearly that As atoms segregate to the growing Ge surface. The amount of segregated As has been found to increase with increasing growth temperature.<sup>3-5</sup>

While it is clear Ge forms ordered overlayers on GaAs(110), the growth mode at various coverages are not clear. Due to the almost perfect lattice match, LEED is unable to distinguish the Ge and GaAs contributions during the initial states of growth and definitive statements cannot be made regarding the growth mode from LEED. Likewise, complications arising from the segregation of substrate atoms prevent conclusive identification of the growth mode using AES and photoemission.<sup>9</sup> While various reconstructions have been reported for thick Ge films under different growth conditions,<sup>3,4,6</sup> the surface structures and the relation among the different reconstructions are still not known.

Scanning tunneling microscopy (STM) provides real space information about the surface morphology, and the Ge/GaAs(110) growth mode and subsequent growth structure can be obtained with ease. In the preceding pa-

per,<sup>10</sup> we showed that isotropic islands as large as  $\sim 10$  monolayers (ML) in height nucleate upon deposition of Ge at 420°C. This paper focuses on the postnucleation growth of Ge and GaAs(110). This growth consists of two parts. The first involves static coalescence of the crystalline Ge islands so that growth proceeds mainly in the lateral dimensions. Such growth leads to networks of Ge islands and, eventually, to complete coverage of the GaAs(110) surface. For Ge deposition exceeding 10 ML, the surface is that of Ge(110) and the growth becomes that of Ge on Ge(110) with some segregated As atoms from the substrate. The energetics at these higher coverages favor layer-by-layer growth with anisotropic islands elongated along  $[1\bar{1}0]$ . We demonstrate that such growth can be altered by either lowering the growth temperature or by increasing the deposition rate. Either change yields a rough surface with isotropic islands. Postannealing of the as-grown surface demonstrates that the smooth surface with elongated islands is thermodynamically preferred. From our STM images, we have identified building blocks for the various surface reconstructions observed here and previously.<sup>3,4,6</sup> A specific surface structure model consisting of As zigzag chains and As dimer chains is proposed.

### EXPERIMENT

Our experiments were performed in an UHV chamber containing a commercial STM (Ref. 11) and LEED optics. The operating pressure was  $\sim 5 \times 10^{-11}$  Torr. Clean GaAs(110) surfaces were obtained by cleaving of  $2 \times 3 \times 8$  mm<sup>3</sup> posts that were Zn doped at  $3 \times 10^{18}$  cm<sup>-3</sup>. Heating of the surface was achieved by radiation from a W filament behind the sample holder. The temperature of the sample was monitored with an infrared pyrometer. Ge was evaporated from W baskets and condensed on the hot GaAs substrates. The amount of metal deposited,  $\theta$ , is expressed in units of monolayers which is defined as the surface atom density of GaAs(110),  $8.86 \times 10^{14}$  cm<sup>-2</sup>, and corresponding to 2.01 Å of Ge. Ge depositions less than 10 ML were achieved by timed exposures to the source after a stable evaporation rate had been established. The deposition rates and amounts for thicker films were deter-

mined directly using a water-cooled quartz crystal thickness monitor. The sample heater was shut off immediately following deposition, and the sample was cooled quickly to room temperature for STM imaging. STM images were acquired in the constant current mode with a typical tunneling current of 0.2 nA. Unless otherwise noted, the STM images reproduced here are oriented so that the  $[1\bar{1}0]$  of the (110) surface runs from the upper-left to the lower-right corner.

## RESULTS AND DISCUSSION

### Coalescence of Ge islands: $\theta < 10$ ML

Figures 1(a) and 1(b) show  $1400 \times 1400 \text{ \AA}^2$  STM scans following depositions of 0.6 and 0.8 ML of Ge at  $420^\circ\text{C}$ . Even at these low coverages, coalescence of Ge islands is clearly evident as the island densities decrease with increasing coverage and are lower than those produced at lower coverages.<sup>10</sup> By 2 ML deposition, cluster coalescence becomes the dominant growth mechanism. Figure 2(a) shows Ge islands that are captured in different stages of coalescence and a closeup view is shown in Fig. 2(b) ( $420 \times 420 \text{ \AA}^2$ ). The cluster labeled *A* is derived from two clusters of different size. Cluster *B* represents an advanced stage of coalescence as the diameter of the neck between the two small clusters approaches the diameter of the original clusters. Cluster *C* shows the coalescence of three distinct entities with two in their later stages of coalescence having made contact with the third cluster.

The driving force for coalescence arises from the fact that regions of high curvature, such as the neck, have a higher surface free energy than regions of low curvature.<sup>12-14</sup> The result is a flow of atoms toward the neck region from other parts of the aggregate. Kinetic factors, such as how the clusters come in contact and how the atoms are transferred to the neck, determine the nature of a coalescence process.

Coalescence involving stationary clusters is referred to as "static." Dynamic coalescence occurs when mobile clusters meet.<sup>12</sup> To examine the nature of Ge island coalescence during deposition, we deposited 4 ML of Ge at  $420^\circ\text{C}$ , imaged the resulting surface, and then annealed it at  $420^\circ\text{C}$  for 30 min. Figures 3(a) and 3(b) show  $1400 \times 1400 \text{ \AA}^2$  STM scans before and after annealing. The absence of noticeable changes indicates that the Ge

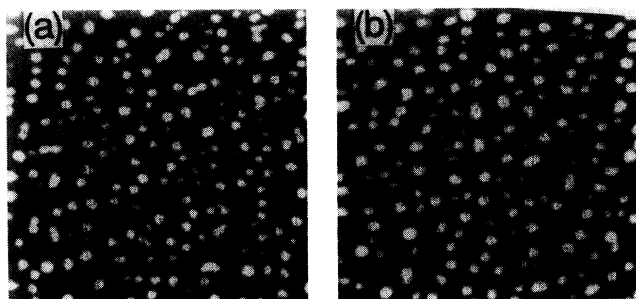


FIG. 1. (a) and (b)  $1400 \times 1400 \text{ \AA}^2$  STM images showing the surface morphology that results from the deposition of 0.6 and 0.8 ML of Ge at  $420^\circ\text{C}$ .

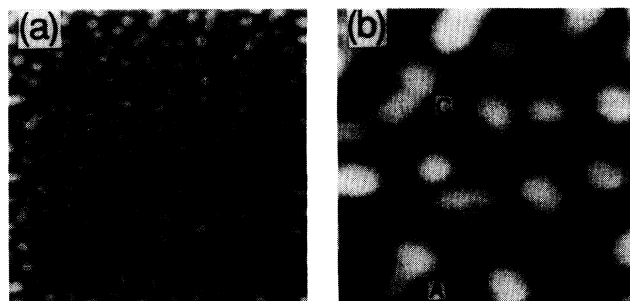


FIG. 2. (a)  $1400 \times 1400 \text{ \AA}^2$  image obtained after 2 ML deposition of Ge at  $420^\circ\text{C}$ . At this stage, coalescence events dominate over island nucleation. (b) A closeup of (a) ( $420 \times 420 \text{ \AA}^2$ ) showing the shapes of clusters that were captured at different stages in the coalescence process.

clusters were not mobile at the growth temperature. Hence coalescence is of static type.

At this 4-ML coverage, the islands were  $\sim 10$  ML in height and island growth proceeded primarily in the lateral direction (coalescence). Figure 3(c) shows a closeup of the overlayer structure. Islands that are not in the process of coalescing, such as *A*, exhibit an isotropic shape with a flat top, as observed for lower deposition.<sup>10</sup> For islands involved in coalescence, the tops of the initial islands remain flat but the next region is lower in height. For island *B*, the neck range is  $\sim 1$  ML lower. These observations demonstrate that flat island tops are thermodynamically preferred.

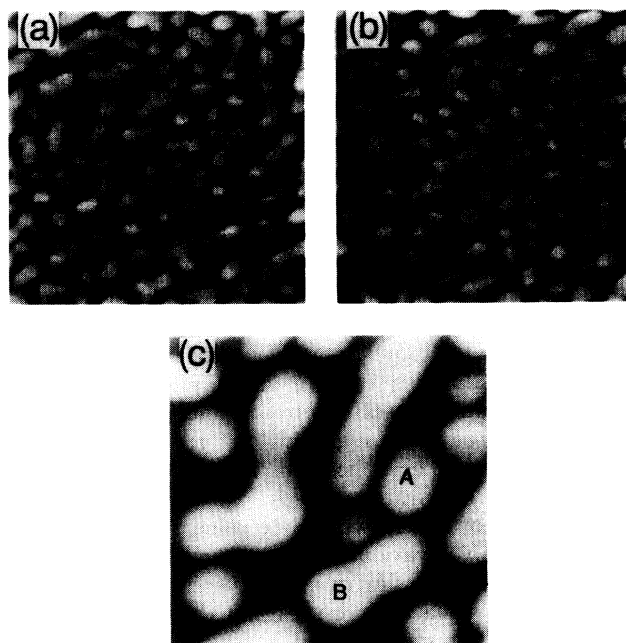


FIG. 3. (a) and (b)  $1400 \times 1400 \text{ \AA}^2$  images following 4 ML Ge deposition showing the as-grown structures at  $420^\circ\text{C}$  and those obtained after annealing at  $420^\circ\text{C}$  for 30 min. The absence of significant differences indicates that the clusters are not mobile at this temperature. (c)  $560 \times 560 \text{ \AA}^2$  image of the surface showing the shapes of coalescing Ge islands.

Although coalescence is driven by thermodynamics, atoms must be transported to the neck region from other parts of the island, and it is important to examine the kinetics associated with the process. During coalescence, the islands can retain their crystalline form and mass transfer is accomplished via surface diffusion, involving little overall island movement. The solid-solid coalescence is expected to be a slow process. In contrast, liquid-liquid coalescence, as in the merging of water droplets, involves both surface and bulk diffusion and there is significant movement of the initial clusters. This process can occur on a relatively short time scale so that the equilibrium shape is always reached before the next coalescence event starts.<sup>15</sup> The observation of elongated islands in Fig. 3 indicates that new coalescing events are initiated before the previous coalescence is complete, consistent with the slowness of solid-solid coalescence. In such a case, the kinetics associated with Ge island coalescence involve diffusion of Ge atoms on Ge clusters, as well as on the GaAs surface. The observation of elongated islands provides further evidence that the Ge clusters are not mobile at the growth temperature.

Figure 4(a) is a  $1400 \times 1400 \text{ \AA}^2$  image for 4 ML Ge/GaAs(110), as in Fig. 3(a), but after annealing at  $585^\circ\text{C}$  for 20 min. The most obvious difference is that the islands have become very large. For example, island A is  $\sim 1000 \text{ \AA}$  by  $\sim 250 \text{ \AA}$  and its height is  $\sim 11$  ML. Unfortunately, the surface was very difficult to image because of the large island height and there is obvious double tip effect. Nevertheless, Fig. 4(a) clearly shows that the tops of the islands are flat and smooth. Since there had been no addition of Ge, the islands probably grew through dynamic coalescence involving the collision of mobile clusters. Even though the clusters were mobile at  $585^\circ\text{C}$ , the fact that elongated islands are observed suggests that the islands remain solid during (solid-solid) coalescence.

Figure 4(b) shows a STM image taken from the same surface as in Fig. 4(a) but with multiple tips. The multiple tip effect is evident as many islands appear to be superimposed. Due to multiple tips, many more islands were sampled than were evident in the same size scan of

Fig. 4(a). In this image, the islands show flat tops with many linear chains along  $[1\bar{1}0]$ . (These linear chains are probably a result of substrate atom segregation to the surface, as discussed below.) The island edges appear to be very sharp, demonstrating that the island structure is driven by thermodynamic forces that favor exposure of specific faces, such as (110). Figure 4(b) shows many small isotropic islands in addition to the large elongated islands of Fig. 4(a). The small islands reflect the coalescence of islands that were close to each other while the elongated large islands were produced by a sequence of coalescent events involving a large number of clusters extended over long distances on the substrate. Elongated islands persist because it is more difficult for given kinetics to transfer the mass necessary to approach the equilibrium configuration, i.e., to produce an isotropic structure for this large island.

Energetically, a system energy versus island dimension curve can be constructed to show that the driving force to adjust the lateral dimension toward equilibrium decreases as the volume of the island increases, as in the preceding paper.<sup>10</sup> Hence the approach to the isotropic shape for large islands is expected to be a slow process both kinetically and energetically. We note that *in situ* scanning-electron-microscopy (SEM) observations for Au deposition on graphite have shown that the coalescence of Au clusters produces elongated aggregates upon annealing at  $50^\circ\text{C}$  for several minutes while isotropic clusters were obtained only after annealing at  $450^\circ\text{C}$  for 100 h.<sup>16</sup>

In the discussion of 0.2 ML Ge/GaAs(110) in paper I, we showed that atomic steps act as preferred nucleation sites.<sup>10</sup> Such surface defects continue to play a significant role during coalescence because of the larger density of clusters at step edges. The mosaic image of Fig. 5 was obtained in a stepped region following the deposition of 4 ML of Ge at  $420^\circ\text{C}$ . This image was obtained near where Fig. 3(a) was produced. Each image making up the mosaic is  $1400 \times 1400 \text{ \AA}^2$ . Two lines decorated with Ge islands extend across the image and a section of a third is also visible. Coalescence at this growth temperature ( $420^\circ\text{C}$ ) is static and it depends on the local cluster density and

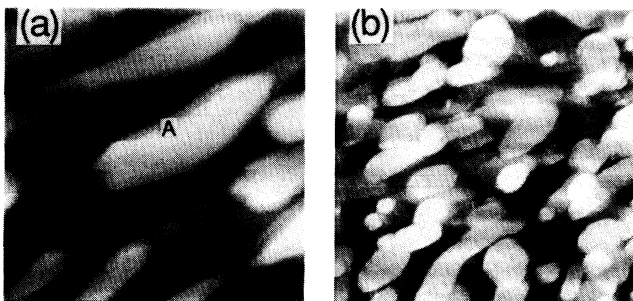


FIG. 4. (a)  $1400 \times 1400 \text{ \AA}^2$  image obtained after the deposition of 4 ML Ge at  $420^\circ\text{C}$  but then annealed at  $585^\circ\text{C}$  for 20 min. (b)  $1400 \times 1400 \text{ \AA}^2$  image of the same surface as (a) showing flat island tops with linear chains along  $[1\bar{1}0]$  (from upper left to lower right) but also pronounced ghosts due to multiple tip effects.



FIG. 5. A mosaic of images taken after 4 ML Ge deposition at  $420^\circ\text{C}$  showing preferential island coalescence along step edges.

the addition of adatoms. Thus, it is not surprising to see that island growth at 4 ML of Ge proceeds preferentially along step edges. A depletion zone can also be seen on both sides of the steps.

An increase in the nominal Ge coverage to 7 ML resulted in a networklike structure rather than the equilibrium shape because of the slow process associated with static solid-solid coalescence. The initiation of new coalescing events before the completion of previous events yields the network structure and growth. This coverage range involves movement in the lateral dimension. The formation of the network structure also creates a thermodynamic demand for the filling of holes in the network as they represent regions with high curvature. The flow of atoms into those holes further limits growth in the vertical direction. This explains the observation that the Ge islands remain  $\sim 10$  ML in height throughout the coalescing process for  $1 < \theta < 10$  ML.

#### Layer-by-layer growth and kinetic effects: $\theta \geq 20$

For coverages greater than  $\sim 10$  ML, the GaAs(110) substrate is completely covered by the Ge and growth represents Ge on Ge(110). Figure 6(a) shows a STM image taken after deposition of 20 ML at a rate of 0.9 ML/min at 420°C where layer-by-layer growth is evident.<sup>17,18</sup> The surface consists mainly of two Ge layers

with the lower layer being nearly complete and the upper layer consisting of anisotropic islands of 2 Å height with elongation along  $[1\bar{1}0]$ . In contrast to isotropic clusters observed at lower coverages, the islands associated with this layer-by-layer growth are highly anisotropic. The smoothness of the surface reflects the fact that the Ge surface diffusion is sufficiently fast at this growth temperature and the arrival rate of adatoms is relatively slow so that the morphology approximates the equilibrium configuration.

Since growth can be driven away from the thermodynamically preferred form by kinetics, we investigated the effects of increased deposition rate and decreased growth temperature on the surface morphology. Figure 6(b) ( $1400 \times 1400 \text{ \AA}^2$ ) shows a 20-ML Ge film grown by relatively fast deposition of 10 ML/min, resulting in a rough surface where 4–5 Ge layers are exposed. The island shape associated with this rough surface is isotropic, in contrast to the slow deposition condition where the islands are elongated. Figure 6(c) shows a  $700 \times 700 \text{ \AA}^2$  STM image following deposition of 20 ML at 350°C at 1 ML/min. Again, a rough surface with isotropic islands is observed. Hence the surface roughness and island shape can be modified by changing the growth condition and, therefore, the kinetics. Furthermore, there is a clear correlation between surface roughness and island shape. Despite these changes, the surface reconstructions remain unchanged, as shown below, ensuring that the morphological differences are due to kinetic effects.

To explain the correlation between surface roughness and island shape anisotropy, we first examine growth on a vicinal surface. Under conditions of high growth temperatures and slow deposition rates, adatoms that impinge on a terrace can diffuse until being incorporated at step edges, as depicted in Fig. 7(a). This step flow mode produces highly anisotropic growth but with little increase in surface roughness. In contrast, under conditions of high deposition rates, adatoms can nucleate islands on the terrace without reaching step edges, as sketched in Fig. 7(b). In this case, the surface roughness

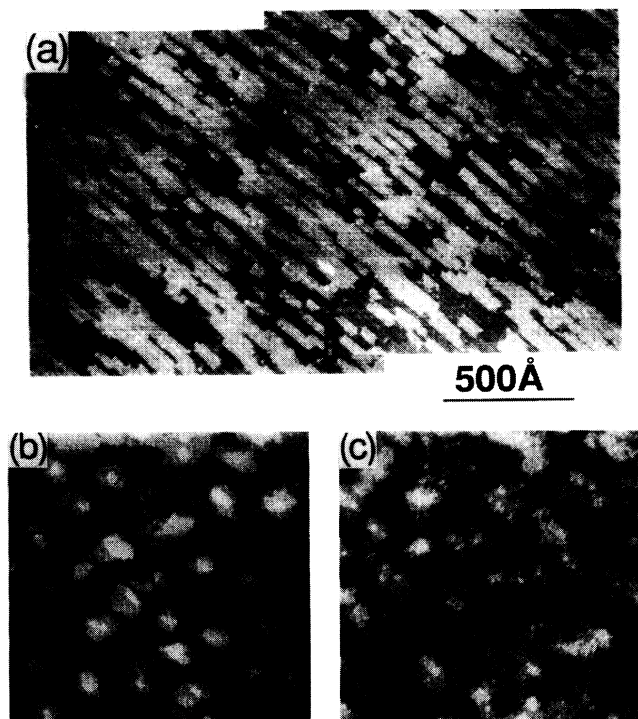


FIG. 6. (a) A mosaic of images for 20 ML Ge deposited at a rate of 0.9 ML/min showing layer-by-layer growth with anisotropic islands. (b)  $1400 \times 1400 \text{ \AA}^2$  image for 20 ML deposition at a rate of 10 ML/min and a temperature of 420°C. These conditions produce a rough surface with isotropic islands. (c)  $700 \times 700 \text{ \AA}^2$  image for 20 ML deposition at a rate of 1 ML/min at 350°C. Comparison to (b) shows the same rough surface with isotropic islands, but much worse surface ordering.

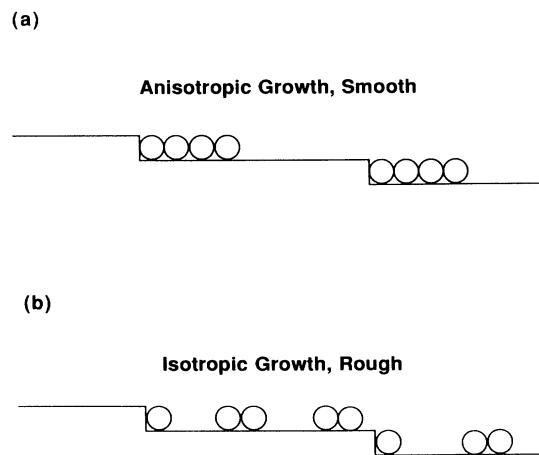


FIG. 7. Schematics showing anisotropic growth that results in a smooth surface (a) and isotropic growth resulting in a rough surface (b).

will increase as the growth proceeds and growth will be more isotropic. Hence surface roughness and growth anisotropy are closely correlated for growth on vicinal surfaces.

For Ge/GaAs(100), our results show that [001] island edges grow much faster than  $[1\bar{1}0]$  edges for slow deposition rates. If this growth anisotropy is a consequence of diffusion being much faster along  $[1\bar{1}0]$  than [001], then an adatom impinging on an island will be more likely to move along  $[1\bar{1}0]$  until it reaches the [001] edge. The result will be a smooth surface with islands elongated along  $[1\bar{1}0]$ , as observed in Fig. 6(a). With increased deposition rates, the adatoms are likely to form new islands on top of existing islands before reaching [001] edges. Hence the effects of anisotropy in diffusion are suppressed and the surface will be more isotropic than one produced under conditions of slow deposition. The effect of decreasing the growth temperature would be an overall reduction in adatom diffusion so that lower growth temperatures would be equivalent to faster deposition. Thus the lower temperature has a similar effect as fast deposition in terms of roughness and isotropy, consistent with morphology shown in Fig. 6(c). Similar arguments can be made by assuming that the kinetic anisotropy arises from differences in the sticking probabilities for adatoms at [001] and  $[1\bar{1}0]$  island edges.

The correlation between surface roughness and island shape anisotropy is important in understanding the role of kinetics. Recent theoretical studies of kinetic growth have also suggested such correlation.<sup>19</sup> A detailed discussion of such correlation and comparison of the experimental results to the kinetics roughening theory has been presented in a previous publication.<sup>20</sup>

From Fig. 6(c), it is clear that the surface ordering is much worse for growth at 350°C than at 420°C [Fig. 6(b)], consistent with differences in Ge mobility. Chen, Bolmont, and Sebenne<sup>6</sup> have reported epitaxial growth of Ge/GaAs(110) at temperatures as low as 160°C based on the observation of a LEED pattern. Our attempts to grow Ge at 350°C or lower always resulted in a film with poor quality, as in Fig. 6(c), even though a LEED pattern was observed. From the surface morphology shown in Fig. 6(c), we conclude that the films grown at low temperature are of poor crystal quality.

#### 20-ML Ge/GaAs(110): Effects of annealing

As we have shown, growth structures are often driven far away from the equilibrium structure by kinetics. Annealing should enhance the relaxation toward the equilibrium configuration. Figure 8(a) shows the same surface as in Fig. 6(b) after annealing at the growth temperature of 420°C for 60 min. Clearly, this surface is much smoother, the islands are much larger, and there is no large anisotropy in island shapes. Further annealing at 525°C for 60 min resulted in a surface that was very smooth, consisting of only two layers [Fig. 8(b)]. Comparing Figs. 8(a) and 8(b) shows that the islands of the top layer have coalesced, forming a networklike structure. Although the islands are now anisotropic, the degree of anisotropy is not as great as for the surface grown under

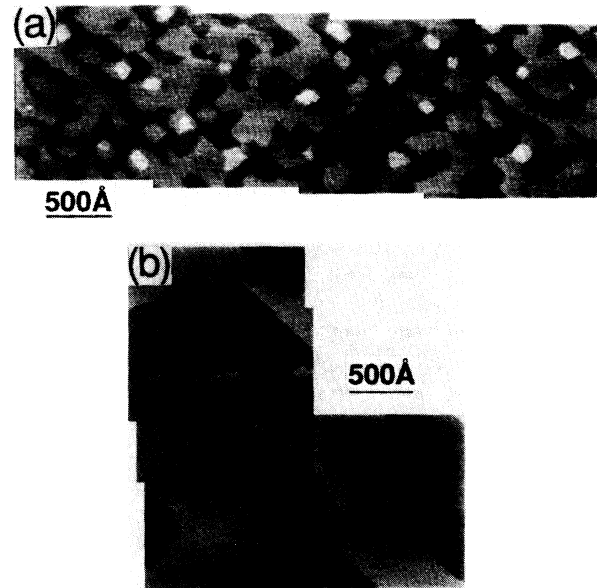


FIG. 8. (a) A mosaic of images taken after annealing the surface shown in Fig. 6(b) at 420°C for 60 min that demonstrates that the surface becomes much smoother but also that the islands remain isotropic. (b) A mosaic of images obtained following additional annealing at 525°C for 60 min that demonstrates the production of a smooth surface with anisotropic islands.

slow deposition conditions [Fig. 6(a)]. Similar differences between growth shapes and equilibrium shapes have also been reported for Si growth on Si(001) where the growth shape has a larger anisotropy than the island shape produced by annealing.<sup>21</sup>

The sequence of annealing experiments for Ge/GaAs(110) demonstrates that a flat surface is preferred thermodynamically over a surface derived from many different layers. Moreover, the change toward the smooth surface upon annealing seems to be much faster than the change from isotropic islands to elongated islands. This slow change from isotropic to anisotropic islands does not suggest that the energy difference between the two island edges is small, but rather is a result of the thermodynamic nature of the islands. To show this, we model a Ge island by a parallelepiped so that the free energy is

$$\begin{aligned} E &= a_x a_y \sigma_1 + 2h(a_x \sigma_x + a_y \sigma_y) \\ &= \sigma_1 V/h + 2h(a_x \sigma_x + a_y \sigma_y), \end{aligned} \quad (1)$$

where  $a_x$ ,  $a_y$ , and  $h$  are the dimensions of the island, inset of Fig. 9(a), and  $\sigma_x$  and  $\sigma_y$  are the free energies associated with the faces of the island.  $\sigma_1$  is equal to  $\sigma_0 + \sigma_i - \sigma_s$ , where  $\sigma_0$  and  $\sigma_s$  are the surface free energies for the overlayer and the substrate and  $\sigma_i$  is the interfacial free energy.

Figure 9(a) plots the  $E$  as a function of island height  $h$  for situations in which a smooth surface is preferred, i.e.,  $\sigma_1 < 0$ . For simplicity, we have assumed  $\sigma_x = \sigma_y = -2\sigma_1$ ,  $a_x = a_y$ , and the cluster volume  $V = 8 \times 10^4 \text{ \AA}^3$ . As shown, the free energy of the island decreases rapidly as

the island height decreases, reaching a minimum in the limit of this continuous model when the island thickness is a single layer. Each monolayer reduction between six and one layers corresponds to a decrease in free energy by more than a factor of 2, representing a large driving force to reduce the island height. In addition, it is clear from the slope of the curve that this driving force increases as the system approaches the lowest-energy configuration, i.e., the single layer height. Accordingly, the reduction of island height should be a very fast process, as observed.

Equation (1) can also be used to address the issue of island anisotropy. To emphasize the lateral change of the island, we assume a constant height  $h$  so that  $a_x/a_y$  is a measure of the anisotropy. The first term on the right of Eq. (1) is then a constant that can be neglected. Figure 9(b) shows the free energy  $E$  as a function of  $a_x/a_y$  for  $\sigma_y/\sigma_x=2$  and 4. The minima in Fig. 9(c) occur when

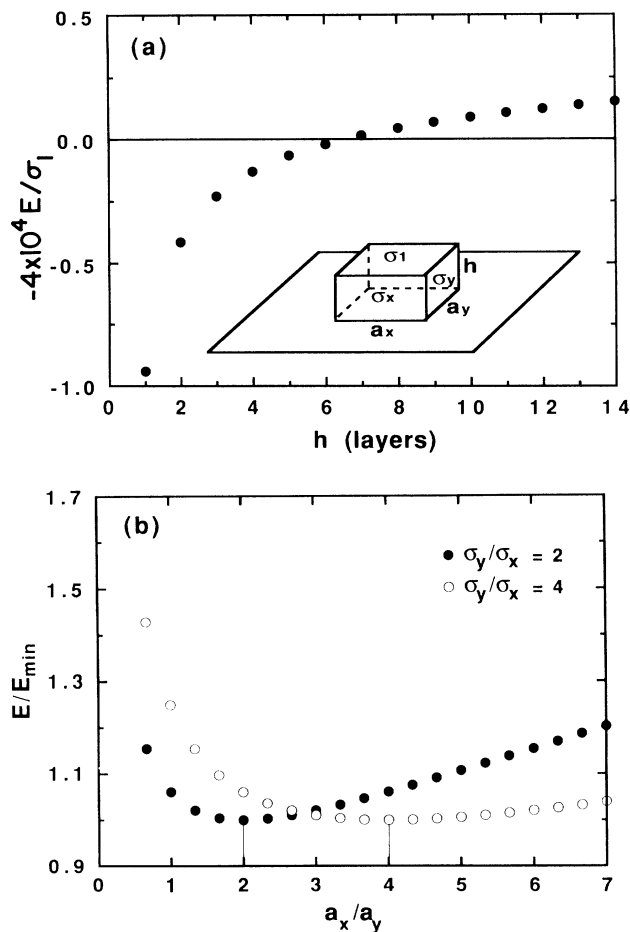


FIG. 9. (a) Plot of calculated energy change as a function of island height for  $\sigma_1 < 0$  showing that the system energy decreases rapidly as the island height decreases. The inset defines the island shape used in the calculation. (b) The plot of energy vs the ratio  $a_x/a_y$  for  $\sigma_1 > 0$  showing that the change from isotropic islands,  $a_x/a_y = 1$ , to anisotropic islands is a slow process despite large energy differences between  $\sigma_x$  and  $\sigma_y$ . The slowness in changing the shape anisotropy is consistent with the evolution of Ge islands upon annealing.

$a_x/a_y = 2$  and 4. The change from isotropic islands ( $a_x/a_y = 1$ ) to the minimum energy configurations involves an energy reduction of only 7% for  $(a_x/a_y)_{\min} = 2$  and 24% for  $(a_x/a_y)_{\min} = 4$ . The driving force toward the equilibrium configurations is then much smaller than that of reducing island height. From the changes in slopes of these curves, it is also clear that the driving forces decrease as the system approaches the minimum energy configuration. Therefore, from a thermodynamic point of view, the evolution of the island shape toward its equilibrium configuration is expected to be a slower process than the reduction of island height. In reality, kinetics also favor height changes over shape changes since atoms in the top layer need only to move short distances to fall to the next layer while the diffusion distances required to change from isotropic to anisotropic shapes are much larger.

#### Surface reconstruction and As segregation

Figures 10(a) and 10(b) are closeup images ( $300 \times 300 \text{ \AA}^2$ ) that show the surface after slow and fast deposition of 20-ML Ge on GaAs(110) at  $420^\circ\text{C}$ . Despite differences in roughness and island shapes, the two surfaces have the same atomic structure. In these images where the filled states are probed, there is ordering that consists of alternating lines of continuous chains and lines of dots along  $[\bar{1}\bar{1}0]$ . The nearest distance between linear chains is  $\sim 17 \text{ \AA}$ , three times the unreconstructed unit-cell dimension of

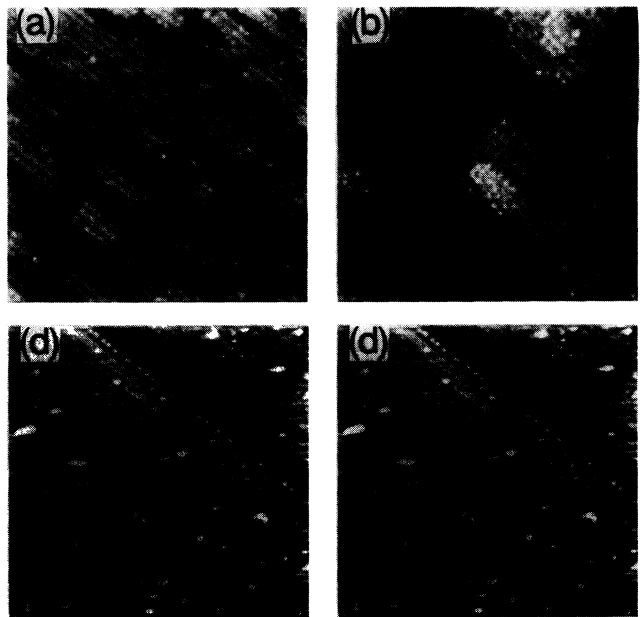


FIG. 10. (a)–(d)  $300 \times 300 \text{ \AA}^2$  STM images of 20 ML Ge/GaAs(110) showing atomic structures of the surface following (a) deposition at  $420^\circ\text{C}$  at a rate of 0.9 ML/min; (b) deposition at  $420^\circ\text{C}$  at a rate of 10 ML/min; (c) annealing of (b) at  $420^\circ\text{C}$  for 60 min; and (d) additional annealing at  $525^\circ\text{C}$  for 60 min. From these images it is clear that the building blocks for the surface structures are continuous linear chains and dotted lines, both along  $[\bar{1}\bar{1}0]$ . In addition, the  $[\bar{1}\bar{1}0]$  island shapes are always terminated with dotted lines.

Ge(110) in [001], 5.6 Å. This spacing is consistent with the observation of a "1×3" LEED pattern.<sup>3-5</sup> Another interesting feature in both Figs. 10(a) and 10(b) is that the island edges are always terminated by dotted line structures. The separation between two dots along [1 $\bar{1}$ 0] is 8 Å, on average, twice the unreconstructed unit-cell dimension. The observed spacing suggests the formation of dimer-type structure so that the true surface reconstruction is 2×3 instead of 1×3. Only very weak and diffuse intensities appeared at half-order spot positions in our LEED pattern, probably because those dimers lacked long-range order.

Figure 10(c) was obtained following annealing of the surface in Fig. 10(b) at the growth temperature of 420°C for 60 min. Significantly, the surface reconstruction remained the same despite the dramatic change in the surface roughness and island size.

Previous Auger and photoemission studies<sup>4-8</sup> of Ge/GaAs(110) have shown the persistence of a strong As signal while the Ga signal became barely detectable by 20 ML deposition. These results demonstrate preferential As surface segregation. For thick Ge films grown at 395°C, the amount of As on the Ge surface has been estimated to be 0.65±0.25 ML and the amount has been shown to increase with increasing growth temperature.<sup>4,5</sup> We then infer that the surface structure shown in Fig. 10 involves As atoms on the Ge(110) surface with a reconstruction that depends on the amount of As present.

To establish a correlation between the As surface concentration and the surface features observed in STM, we annealed the 20-ML Ge film at 585°C for 60 min. This resulted in a 2×5 LEED pattern instead of the 2×3 pattern for the as-grown surface at 420°C. The STM image of Fig. 10(d) shows that the building blocks for the 2×5 structure are the same as 2×3, consisting of linear chains and dotted lines. The difference is that the reconstructed unit cell in [001] consists of two linear chains and one dotted line for 2×5. The increase in the number of linear chains coincides with an increased amount of segregated As on the surface upon annealing to high temperature.<sup>3,5,8</sup> We conclude that the linear chains are richer in As than the dotted lines.

Figure 11(a) shows dual-image STM results that probe the occupied and unoccupied densities of states simultaneously. The points labeled *A* and *B* identify identical locations in the two images. The linear chains appear as bright protrusions in the occupied state image and as dark depressions in the unoccupied state image while the dotted lines appear as protrusions in both images. Measurements of surface heights in the occupied image show no significant difference between linear chains and dotted lines, suggesting that both are As-related features.

Figure 11(b) is a schematic of the surface structure that we propose, where the linear chains arise from the zigzag arrangement of As atoms and the dotted lines correspond to dimerized As adsorption on Ge surface atoms. Each As atom in the As zigzag chains is bonded to two neighboring As atoms and back-bonded to a Ge atom. In this configuration, an As atom contributes one electron each to the As-As and As-Ge bonds. Since an As atom has five valence electrons, the As dangling bond in this

structure would have two electrons and the dangling bond state would be filled.<sup>22,23</sup> This is consistent with the STM observation that the long linear chains appear as bright features in the filled state image and dark features in the empty state image [Fig. 11(a)]. The observation of a 2×3 LEED pattern and the fact that these linear chains are three lattice spacings apart demonstrate that it is not favorable for the As zigzag chains to be next to one another.

The dotted line structure in the filled state image has a similar appearance in the empty state image (although not as well resolved). While we cannot rule out the possibility that such a feature is due to Ge, this would be unlikely since it is difficult for Ge atoms in the zigzag chain to form dimers. To understand the dotted structure, we first examine the situation at [1 $\bar{1}$ 0] step edges (Fig. 10) where each Ge atom has one dangling bond. Saturation of these dangling bonds with As atoms allows the As atoms to reduce the number of their dangling bonds, thus lowering the surface energy, by forming dimers between

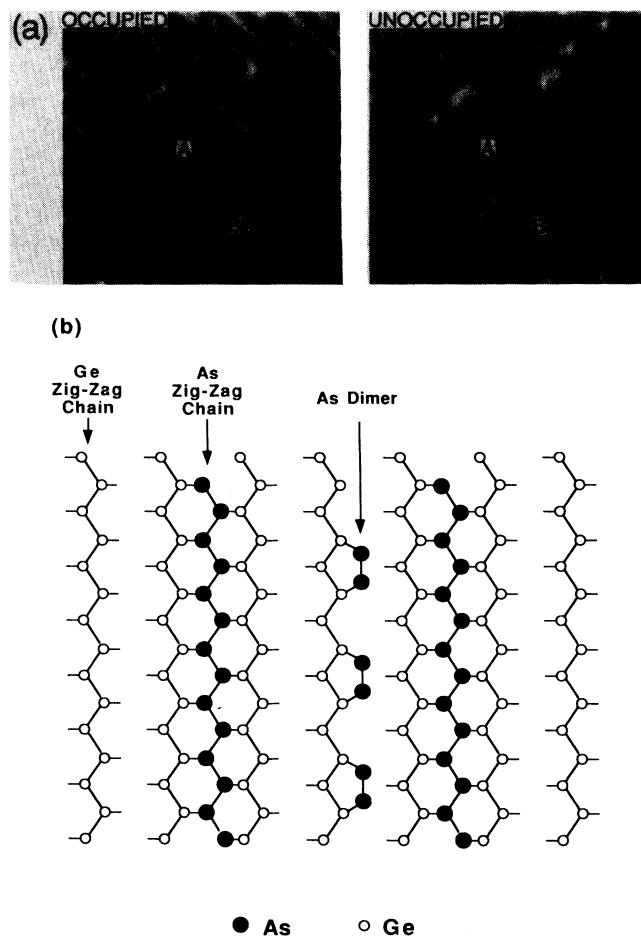


FIG. 11. (a) Dual-bias image of the 3×2 surface for 20 ML Ge/GaAs(110) after annealing at 420°C for 60 min showing that the linear chains appear as bright protrusions in the occupied state image and dark depressions in the unoccupied state image. The dotted lines have the same appearance in both images. (b) Proposed structure for the 3×2 surface, consisting of zigzag arrangements of As and As dimer rows on the Ge(110) surface.

neighboring As atoms. As the dangling bond state of these dimers is neither completely filled nor completely empty, they should appear as dotted lines in both filled and empty images, as experimentally observed. It is evident from the STM images in Fig. 10 that the dotted lines at  $[1\bar{1}0]$  step edges have identical appearance to the dotted lines in the terraces. It is then reasonable to assume that the same structure is responsible for the observed dotted lines in the terraces. As shown in Fig. 11(b), such dimer structures involve As atoms preferentially adsorbed at one type of Ge atom in the Ge zigzag chain. Such preferential sites can arise if the Ge zigzag chains undergo relaxation similar to GaAs(110), as suggested by Chadi's theoretical calculation.<sup>24</sup> In such a case, the As atoms would prefer Ge atoms that are pushed down in position as the dangling bond state for such Ge atoms is empty. Such a dimer structure can be easily converted into an As zigzag chain if the amount of As increases, as is the case when the surface is annealed to 585 °C and the neighboring row of Ge sites (the other type) become occupied by the As atoms. Since the zigzag chains are richer in As than the dimer chains, the increased amount of As is accommodated by converting dimer chains to zigzag chains. This is consistent with the observation of an increase in the linear chains relative to the dotted chains following annealing to high temperature. Finally, we note from Figs. 10(c) and 10(d) that the transformation from  $2 \times 3$  to  $2 \times 5$  requires a coherent rearrangement of linear chains and dotted lines. This indicates that the change of reconstruction involves reminimization of the surface energy as the As concentration increases.

### SUMMARY

We have shown that Ge films grow following initial nucleation through static coalescence at 420 °C. The growth in this coverage range, 1–10 ML, proceeds primarily in the lateral dimension with little change in Ge island height. We have demonstrated that the Ge islands remain solid during coalescence. Coalescence was found to proceed preferentially along step edges because of the high density of initial nucleated Ge islands at step

edges.<sup>10</sup> Such coalescence is a slow process, the isotropic equilibrium island shape was not obtained during growth and coalescence resulted in a networklike structure. The GaAs surface was covered after  $\sim 10$  ML deposition. This type of growth mode establishes a minimum thickness of  $\sim 10$  ML for Ge layers, should Ge-GaAs superlattices be grown at 420 °C.

Deposition beyond 10 ML results in a change in the growth mode to layer by layer as the growth system now is effectively Ge on Ge(110) with segregated As atoms released from the GaAs substrate. Investigations of the effects of kinetics revealed a correlation between the surface roughness and island shape anisotropy. Smooth surfaces with anisotropic islands were obtained by slow deposition at high temperature (420 °C) and rough surfaces with isotropic islands were obtained either by fast deposition at high temperature or slow deposition at low temperature (350 °C). The observed growth morphologies were explained in the context of anisotropic kinetics and the suppression of such anisotropies by the growth condition. Annealing of the as-grown rough surface demonstrated that smooth surfaces (or layer-by-layer growth) with elongated two-dimensional (2D) islands were thermodynamically preferred. We also showed that the driving force to reduce the island height is much larger than that to drive islands to elongated shapes.

For 20-ML coverage or higher, we identified that the building blocks of the surface reconstructions were continuous linear chains and dotted lines, both along  $[1\bar{1}0]$ . Different combinations of these two building blocks easily generate the different reconstructions, such as  $2 \times 3$ ,  $2 \times 5$ , that have been observed in our LEED studies and in previous experiments.<sup>3–5</sup> We found that the  $[1\bar{1}0]$  step edges were terminated with dotted line structure. Based on these observations and dual-bias STM images, we associated the dotted lines with As dimers and continuous dimers with As zigzag chains.

### ACKNOWLEDGMENTS

This work was supported by the Office of Naval Research and the National Science Foundation.

<sup>1</sup>H. Kroemer, *Jpn. J. Appl. Phys. Suppl.* **20**, 9 (1981).

<sup>2</sup>J. H. Weaver, in *A New Era of Materials Science*, edited by J. R. Chelikowsky and A. Franciosi (Springer-Verlag, Berlin, 1991), Chap. 8, and references therein.

<sup>3</sup>W. Mönch and H. Gant, *J. Vac. Sci. Technol.* **17**, 1094 (1980).

<sup>4</sup>W. Mönch, R. S. Bauer, H. Gant, and R. Murschall, *J. Vac. Sci. Technol.* **21**, 498 (1982).

<sup>5</sup>R. S. Bauer and J. C. McMennamin, *J. Vac. Sci. Technol.* **15**, 1444 (1978).

<sup>6</sup>P. Chen, D. Bolmont, and C. A. Sebenne, *J. Phys. C* **15**, 6101 (1982); *Surf. Sci.* **132**, 505 (1983).

<sup>7</sup>R. S. Bauer, R. Z. Bachrach, G. Hansson, and P. Chiaradia, *J. Vac. Sci. Technol.* **19**, 674 (1981).

<sup>8</sup>R. Z. Bachrach and R. S. Bauer, *J. Vac. Sci. Technol.* **16**, 1149 (1979).

<sup>9</sup>E. Bauer and H. Poppa, *Thin Solid Films* **12**, 167 (1972).

<sup>10</sup>Y.-N. Yang, Y. S. Luo, and J. H. Weaver, preceding paper, *Phys. Rev. B* **46**, 15 386 (1992).

<sup>11</sup>Park Scientific Instruments STM-SU2, Mountain View, CA 94089.

<sup>12</sup>R. Kern, in *Interfacial Aspects of Phase Transformations*, Vol. 87 of *NATO Advanced Study Institute, Series C: Mathematical and Physical Sciences*, edited by B. Mutafschiev (Reidel, Dordrecht, 1982), pp. 303–314.

<sup>13</sup>M. Zinke-Allmang, in *Kinetics of Ordering and Growth at Surfaces*, Vol. 239 of *NATO Advanced Study Institute, Series B: Physics*, edited by M. G. Lagally (Plenum, New York, 1990), pp. 455–472.

<sup>14</sup>A. R. Tholen, in *Contribution of Cluster Physics to Materials Science and Technology*, Vol. 104 of *NATO Advanced Study*



- Institute, Series E: Applied Science*, edited by J. Davenas and P. M. Rabette (Nijhoff, Boston, 1986), pp. 601–615.
- <sup>15</sup>Y.-N. Yang, Y. S. Luo, and J. H. Weaver, *Phys. Rev. B* **45**, 3606 (1992) discussed Ag coalescence on GaAs(110) that involved more liquidlike coalescence than observed here for Ge.
- <sup>16</sup>J. C. Heyraud and J. J. Métois, *J. Cryst. Growth* **50**, 571 (1980); *Thin Solid Films* **75**, 1 (1981).
- <sup>17</sup>E. Bauer, *Appl. Surf. Sci.* **11/12**, 479 (1982).
- <sup>18</sup>B. Lewis and J. C. Matthews, *Nucleation and Growth of Thin Films* (Academic, New York, 1978).
- <sup>19</sup>D. E. Wolf, *Phys. Rev. Lett.* **67**, 1783 (1991).
- <sup>20</sup>Y.-N. Yang, Y. S. Luo, and J. H. Weaver, *Phys. Rev. B* **45**, 13 803 (1992).
- <sup>21</sup>M. G. Lagally, Y.-W. Mo, R. Kariotis, B. S. Swartzentruber, and M. B. Webb, in *Kinetics of Ordering and Growth at Surfaces*, Vol. 239 of *NATO Advanced Study Institute, Series B: Physics*, edited by M. G. Lagally (Plenum, New York, 1990), pp. 145–168.
- <sup>22</sup>M. D. Pashley, *Phys. Rev. B* **40**, 10 481 (1989).
- <sup>23</sup>D. J. Chadi, in *The Structures of Surface III*, edited by S. Y. Tang, M. A. Van Hove, L. Takayanagi, and X. D. Xie (Springer-Verlag, New York, 1991), pp. 532–544.
- <sup>24</sup>D. J. Chadi, *Phys. Rev. B* **19**, 2074 (1979).

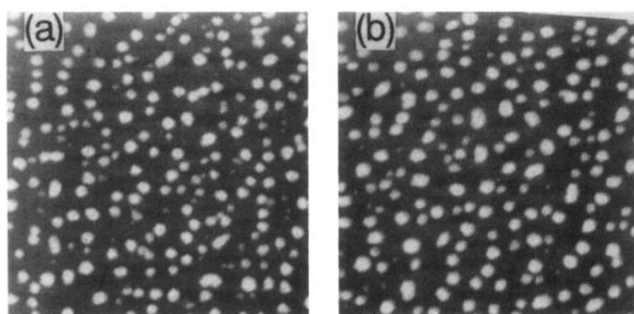


FIG. 1. (a) and (b)  $1400 \times 1400 \text{ \AA}^2$  STM images showing the surface morphology that results from the deposition of 0.6 and 0.8 ML of Ge at  $420^\circ\text{C}$ .

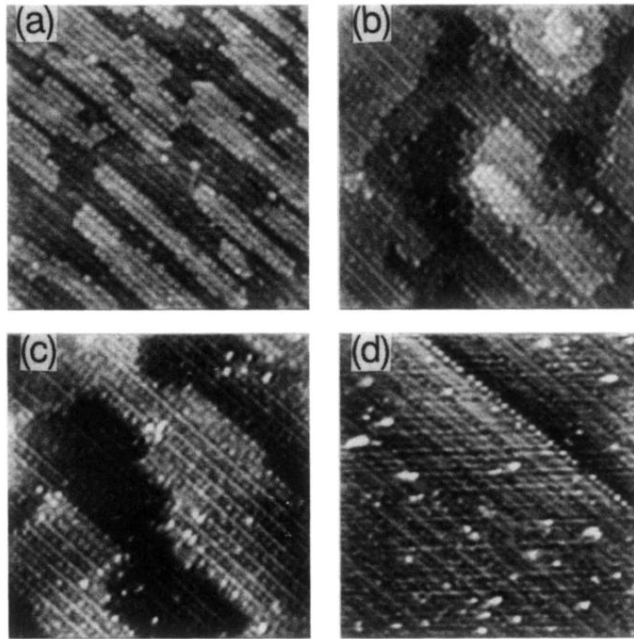


FIG. 10. (a)–(d)  $300 \times 300 \text{ \AA}^2$  STM images of 20 ML Ge/GaAs(110) showing atomic structures of the surface following (a) deposition at  $420^\circ\text{C}$  at a rate of 0.9 ML/min; (b) deposition at  $420^\circ\text{C}$  at a rate of 10 ML/min; (c) annealing of (b) at  $420^\circ\text{C}$  for 60 min; and (d) additional annealing at  $525^\circ\text{C}$  for 60 min. From these images it is clear that the building blocks for the surface structures are continuous linear chains and dotted lines, both along  $[1\bar{1}0]$ . In addition, the  $[1\bar{1}0]$  island shapes are always terminated with dotted lines.

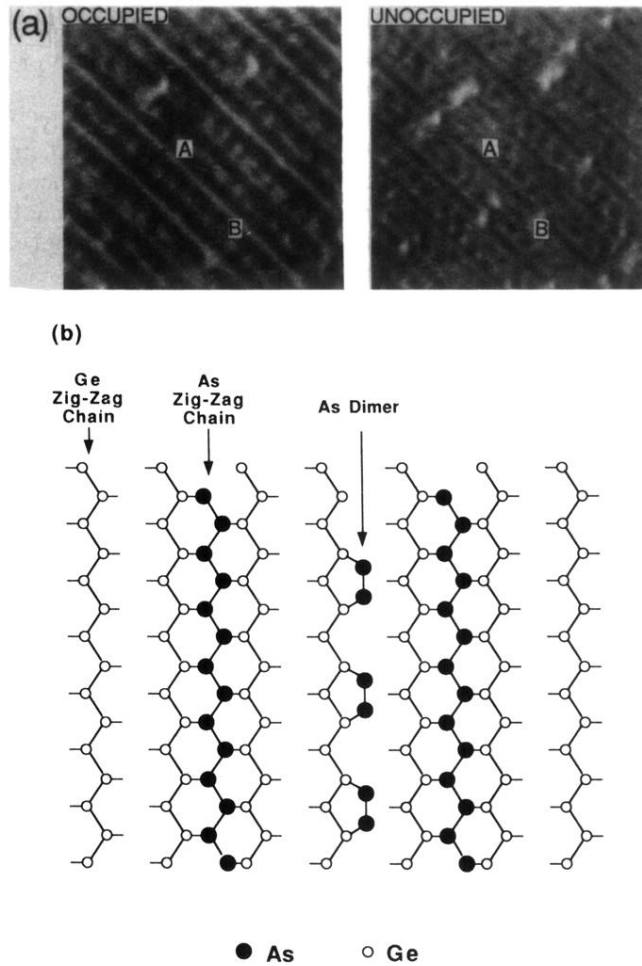


FIG. 11. (a) Dual-bias image of the  $3 \times 2$  surface for 20 ML Ge/GaAs(110) after annealing at  $420^\circ\text{C}$  for 60 min showing that the linear chains appear as bright protrusions in the occupied state image and dark depressions in the unoccupied state image. The dotted lines have the same appearance in both images. (b) Proposed structure for the  $3 \times 2$  surface, consisting of zigzag arrangements of As and As dimer rows on the Ge(110) surface.

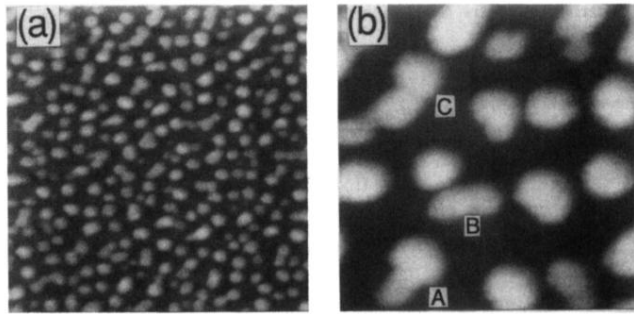


FIG. 2. (a)  $1400 \times 1400 \text{ \AA}^2$  image obtained after 2 ML deposition of Ge at  $420^\circ\text{C}$ . At this stage, coalescence events dominate over island nucleation. (b) A closeup of (a) ( $420 \times 420 \text{ \AA}^2$ ) showing the shapes of clusters that were captured at different stages in the coalescence process.

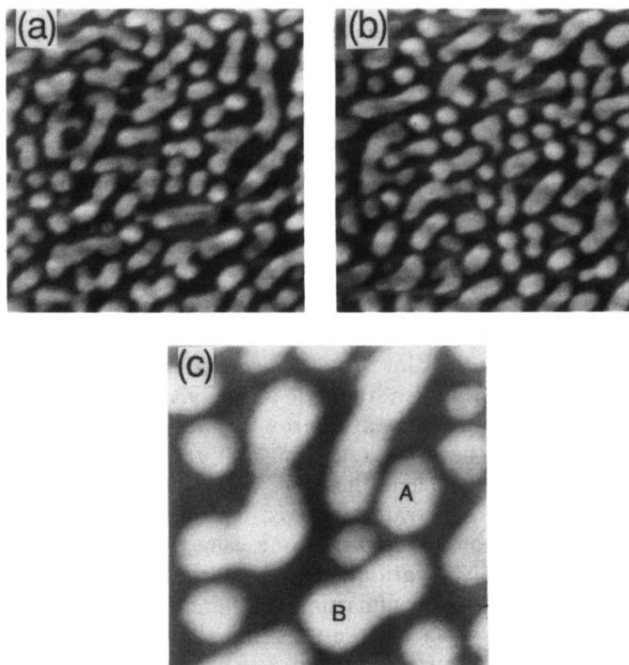


FIG. 3. (a) and (b)  $1400 \times 1400 \text{ \AA}^2$  images following 4 ML Ge deposition showing the as-grown structures at  $420^\circ\text{C}$  and those obtained after annealing at  $420^\circ\text{C}$  for 30 min. The absence of significant differences indicates that the clusters are not mobile at this temperature. (c)  $560 \times 560 \text{ \AA}^2$  image of the surface showing the shapes of coalescing Ge islands.

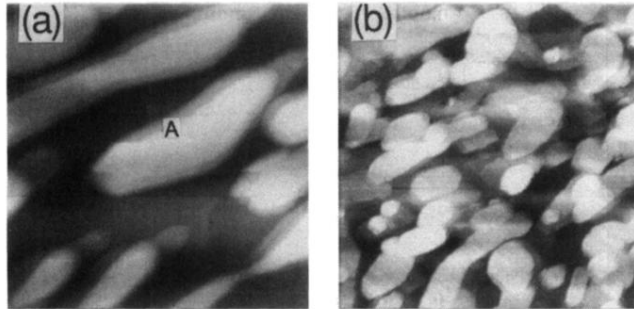


FIG. 4. (a)  $1400 \times 1400 \text{ \AA}^2$  image obtained after the deposition of 4 ML Ge at  $420^\circ\text{C}$  but then annealed at  $585^\circ\text{C}$  for 20 min. (b)  $1400 \times 1400 \text{ \AA}^2$  image of the same surface as (a) showing flat island tops with linear chains along  $[1\bar{1}0]$  (from upper left to lower right) but also pronounced ghosts due to multiple tip effects.

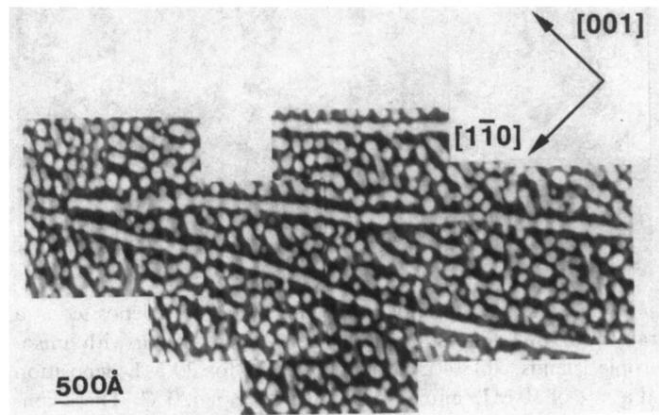
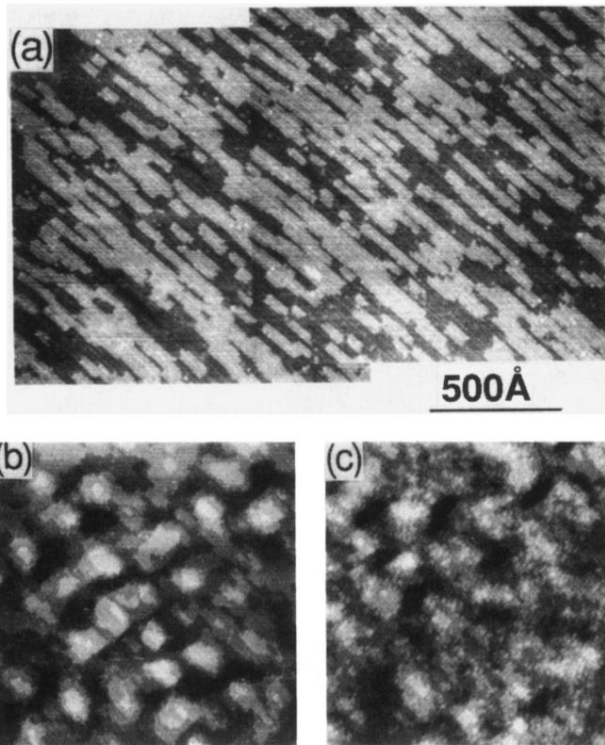


FIG. 5. A mosaic of images taken after 4 ML Ge deposition at 420°C showing preferential island coalescence along step edges.





**FIG. 6.** (a) A mosaic of images for 20 ML Ge deposited at a rate of 0.9 ML/min showing layer-by-layer growth with anisotropic islands. (b)  $1400 \times 1400 \text{ \AA}^2$  image for 20 ML deposition at a rate of 10 ML/min and a temperature of  $420^\circ\text{C}$ . These conditions produce a rough surface with isotropic islands. (c)  $700 \times 700 \text{ \AA}^2$  image for 20 ML deposition at a rate of 1 ML/min at  $350^\circ\text{C}$ . Comparison to (b) shows the same rough surface with isotropic islands, but much worse surface ordering.

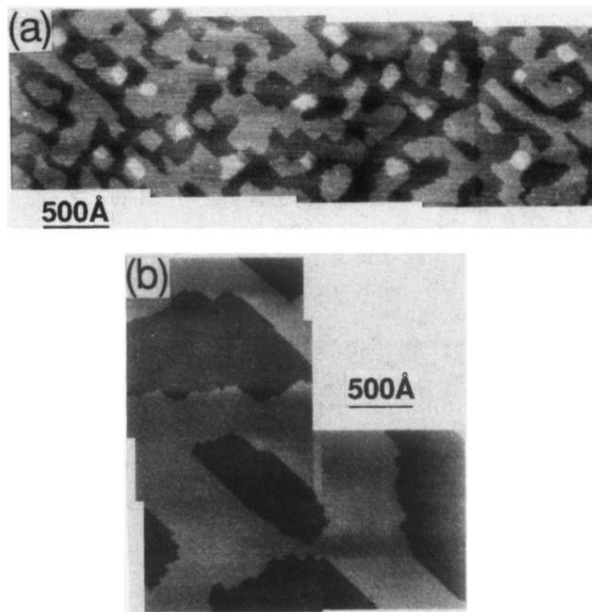


FIG. 8. (a) A mosaic of images taken after annealing the surface shown in Fig. 6(b) at 420°C for 60 min that demonstrates that the surface becomes much smoother but also that the islands remain isotropic. (b) A mosaic of images obtained following additional annealing at 525°C for 60 min that demonstrates the production of a smooth surface with anisotropic islands.